



MULTI-ORDER FRACTIONAL MATHIEU EQUATION WITH EXTERNAL MULTI-PERIODIC EXCITATION

Joshua Ikechukwu Nwamba¹

¹ICT Department, Imo State University

ABSTRACT

This paper presents an investigation of the behavior of the multi-order fractional differential equation (MFDE). We derive expressions for the transition curves separating regions of stability from instability for the MFDE generally and the particular case $k = 2$. Employing the harmonic balance technique, we obtained approximate expressions for the $n=1$ and $n=0$ transition curves of the MFDE and particularly for the case $k = 2$. We also obtained an approximate analytical solution to the multi-order fractionally damped and forced Duffing-Mathieu equation as well as some special cases computationally using the Homotopy Perturbation Method (HPM).

Keywords: Homotopy perturbation method, Parametric excitation, Fractional calculus, Harmonic balancing method, Damping, Fractional mathieu's equation.

Received: 9 September 2016/ Revised: 5 October 2016/ Accepted: 25 October 2016/ Published: 4 November 2016

1. INTRODUCTION

Mathieu's equation as reported in Nwamba [1] has wide applications in Boundary Value Problems (BVPs) and recently it has been practically applied in the following areas: frequency modulation, alternating gradient focusing, the mirror trap for neutral particles, the inverted pendulum, vibrations in an elliptic drum, stability of a floating body and the Paul trap for charged particles. The equation in its original form is given by

$$\frac{d^2\psi}{dt^2} + (\delta + 2\varepsilon \cos 2t)\psi = 0 \tag{1}$$

It was first introduced by Mathieu in Mathieu [2] when he determined the vibration modes of a stretched membrane having an elliptical clamped boundary. Since its introduction, extensive studies have been conducted on/with (1), these studies have revealed the importance of the equation (1) and many of its variation in nonlinear dynamics of real physical systems of engineering and other areas. Reference [1, 3] presented a survey of some of the nonlinear variations of (1), some of which were listed below in (2)-(5). As was noted in Rand [4] Eq. (1) commonly occurs in nonlinear vibration problems in two different ways. These ways were properly described in Rand [4].

$$\frac{d^2\psi}{dt^2} + c \frac{d\psi}{dt} + (\delta + 2\varepsilon \cos 2t)\psi = 0 \tag{2}$$

$$\frac{d^2\psi}{dt^2} + c \frac{d\psi}{dt} + (\delta + 2\varepsilon \cos 2t)\psi = b\psi(t - 2\pi) \tag{3}$$

$$\frac{d^2\psi}{dt^2} + c \frac{d\psi}{dt} \left| \frac{d\psi}{dt} \right| + (\delta + 2\varepsilon \cos 2t)\psi = 0 \tag{4}$$

$$\frac{d^2\psi}{dt^2} + (\delta + 2\varepsilon \cos 2t)\psi + \beta\psi^3 = 0 \tag{5}$$

δ is the transient curve/transition curve, c is the damping coefficient, $\varepsilon \ll 1$ is a small parameter and b is the delay coefficient.

For the summary of works done on these nonlinear variations of (1), see [1]. A detailed analysis of Mathieu’s equation especially that of stability, can also be found in Rand [4]. In all these extensive studies, we note that the fractional aspect of Mathieu’s equation is not left out, see [1, 4-6].

2. THE PROPOSED FRACTIONAL MODEL

Fractional calculus and fractional order differential equations clearly has wide applications in areas like control theory, diffusion, heat conduction, viscoelasticity and electromagnetics. References [1, 4-6] cites numerous works where such applications were discussed. Many fractional differential equations have been extensively discussed and treated recently. We can find a detailed list of such equations in Rand, et al. [5]. On the other hand, though much work have not been done in developing a complete theory of multi-order fractional differential equations, few literatures exist in this regard (see [7-10]). Moreover, the importance of multi-order fractional differential equations cannot be overemphasized in the areas of mathematical physics and engineering, for example the Basset as well as the Bagley-Torvick equations are popular ones. In this work, we shall not go into the theoretical basis underlying fractional calculus, but interested readers can see [11-13].

The aim of this present work is first to, *propose a more general form of the damped fractional Mathieu equation with external periodic forcing (6) and following [5] discuss the effect of the external forcing on the transition curves separating regions of stability from regions of instability in (10)*, secondly, *to obtain an approximate analytical solution to the proposed MFDE (6) and the multi-order fractionally damped and forced Duffing-Mathieu equation using the HPM [14-21]*.

$$D_t^k x(t) + cD_t^\alpha x(t) + (b + d \cos t)x(t) = F_0 \cos \sqrt{bt} + F_1 \sin \sqrt{bt} \tag{6}$$

where $2 \leq k < 3$, $0 < \alpha \leq 1$, $b = n^2 / 4, n = 1, 2, 3, \dots$ is the transient curve/transition curve, c is the damping coefficient, d is the amplitude of the parametric forcing, it is usually small. $F_0 = \beta f_0$ and $F_1 = \lambda f_1$ are the external forcing amplitudes, β, λ being arbitrary constants. Following [6] we define

$$D_t^k x(t) = \frac{d^k x(t)}{dt^k} = \frac{1}{\Gamma(p-k)} \frac{d^p}{dt^p} \int_0^t \frac{x(y)dy}{(t-y)^{1+k-p}} \tag{7}$$

k , the order of the operation is a positive real number and p is an integer that satisfies $p-1 \leq k < p$.

Setting $p = 1$ and $k = \alpha$ in (7), we obtain

$$D_t^\alpha x(t) = \frac{d^\alpha x(t)}{dt^\alpha} = \frac{1}{\Gamma(1-\alpha)} \frac{d}{dt} \int_0^t \frac{x(y)dy}{(t-y)^\alpha} \tag{8}$$

Letting $t - y = w$ in (8), we obtain

$$D_t^\alpha x(t) = \frac{1}{\Gamma(1-\alpha)} \frac{d}{dt} \int_0^t w^{-\alpha} x(t-w)dw \tag{9}$$

We note that setting $k = 2$ in (6) gives the fractional model equation

$$x''(t) + cD_t^\alpha x(t) + (b + d \cos t)x(t) = F_0 \cos \sqrt{bt} + F_1 \sin \sqrt{bt} \tag{10}$$

Also, setting $F_0 = F_1 = 0$ in Eq. (10) gives the fractional model equation (11) studied in Rand, et al. [5].

$$x''(t) + cD_t^\alpha x(t) + (b + d \cos t)x(t) = 0 \tag{11}$$

3. ANALYSIS OF THE PROPOSED FRACTIONAL MATHIEU EQUATION

In this section, we employ the method of harmonic balance to obtain approximate expressions for the transient curves/transition curves $b = n^2 / 4, n = 0, 1, 2, 3, \dots$ in (6). After [5] we put forward a truncated Fourier series in order to obtain an approximation for the $n = 1$ transition curves, thus

$$x(t) = \beta \cos \frac{t}{2} + \lambda \sin \frac{t}{2} + \dots \tag{12}$$

Generally from (7), for $p = 3$ and $m \geq 1$

$$D_t^k \left(\beta \cos \frac{mt}{2} + \lambda \sin \frac{mt}{2} \right) = \frac{1}{\Gamma(3-k)} \frac{d^2}{dt^2} \int_0^t \left[\beta \cos \frac{mq}{2} + \lambda \sin \frac{mq}{2} \right] (t-q)^{2-k} dq \tag{13}$$

Performing the above indicated operation in (13) as $t \rightarrow \infty$ gives

$$D_t^k \left(\beta \cos \frac{mt}{2} + \lambda \sin \frac{mt}{2} \right) = \left(\frac{2}{m} \right)^{-k} \begin{bmatrix} \sin \frac{mt}{2} \left(\beta \sin \frac{(k-2)\pi}{2} - \lambda \cos \frac{(k-2)\pi}{2} \right) \\ -\cos \frac{mt}{2} \left(\lambda \sin \frac{(k-2)\pi}{2} + \beta \cos \frac{(k-2)\pi}{2} \right) \end{bmatrix} \tag{14}$$

We compute the fractional derivative given in (7) from (14) using (12) to obtain the following expression

$$D_t^k x(t) = \frac{1}{2^k} \begin{bmatrix} \sin \frac{t}{2} \left(\beta \sin \frac{(k-2)\pi}{2} - \lambda \cos \frac{(k-2)\pi}{2} \right) \\ -\cos \frac{t}{2} \left(\beta \cos \frac{(k-2)\pi}{2} + \lambda \sin \frac{(k-2)\pi}{2} \right) \end{bmatrix} \tag{15}$$

Using (12) in (9) as well, we obtain the result below. This result was also obtained in Rand, et al. [5].

$$D_t^\alpha x(t) = \frac{1}{2^\alpha} \left[\cos \frac{t}{2} \left(\beta \sin \frac{\alpha\pi}{2} + \lambda \cos \frac{\alpha\pi}{2} \right) + \sin \frac{t}{2} \left(\beta \cos \frac{\alpha\pi}{2} - \lambda \sin \frac{\alpha\pi}{2} \right) \right] \tag{16}$$

Substituting (16), (15) and (12) into (6), collecting like terms and equating to zero coefficients of $\cos \frac{t}{2}$ and $\sin \frac{t}{2}$, we obtain:

$$\sin \frac{t}{2} : \beta \left(\frac{1}{2^k} \sin \frac{(k-2)\pi}{2} + \frac{c}{2^\alpha} \cos \frac{\alpha\pi}{2} \right) = \lambda \left[\left(\frac{1}{2^k} \cos \frac{(k-2)\pi}{2} + \frac{c}{2^\alpha} \sin \frac{\alpha\pi}{2} \right) - (b + d \cos t) \right] + f_1 \tag{17a}$$

$$\cos \frac{t}{2} : \beta \left((b + d \cos t) - \frac{1}{2^k} \cos \frac{(k-2)\pi}{2} + \frac{c}{2^\alpha} \sin \frac{\alpha\pi}{2} \right) = \lambda \left[\left(\frac{1}{2^k} \sin \frac{(k-2)\pi}{2} + \frac{c}{2^\alpha} \cos \frac{\alpha\pi}{2} \right) \right] + f_0 \tag{17b}$$

Eliminating β and λ from equations (17a) and (17b) gives the following approximate expression for the $n=1$ transition curves

$$b = \frac{1}{2} \left[\left(f_1 + f_0 + \frac{1}{2^{k-1}} \cos \frac{(k-2)\pi}{2} - \frac{c}{2^{\alpha-1}} \cos \frac{\alpha\pi}{2} \right) \pm \left[(f_1 - f_0)^2 + 2d(f_1 - f_0) + d^2 - 4 \left(\frac{1}{2^k} \sin \frac{(k-2)\pi}{2} - \frac{c}{2^\alpha} \sin \frac{\alpha\pi}{2} \right)^2 \right]^{1/2} \right] \tag{18}$$

Setting $k = 2$ to obtain the approximate expression for the $n=1$ transition curves for Eq. (10), we have that

$$b = \frac{f_1 + f_0}{2} + \frac{1}{4} - \frac{c}{2^\alpha} \cos \frac{\alpha\pi}{2} \pm \frac{1}{2} \left[(f_1 - f_0)^2 + 2d(f_1 - f_0) + d^2 - \frac{c^2}{2^{2\alpha-2}} \sin^2 \frac{\alpha\pi}{2} \right]^{1/2} \tag{19}$$

This will be the same result obtained for Eq. (11) in Rand, et al. [5] if $f_1 = f_0 = 0$. Figures 1, 2 and 3 displays the transition curves Eq. (19) for various values of f_1, f_0 and α .

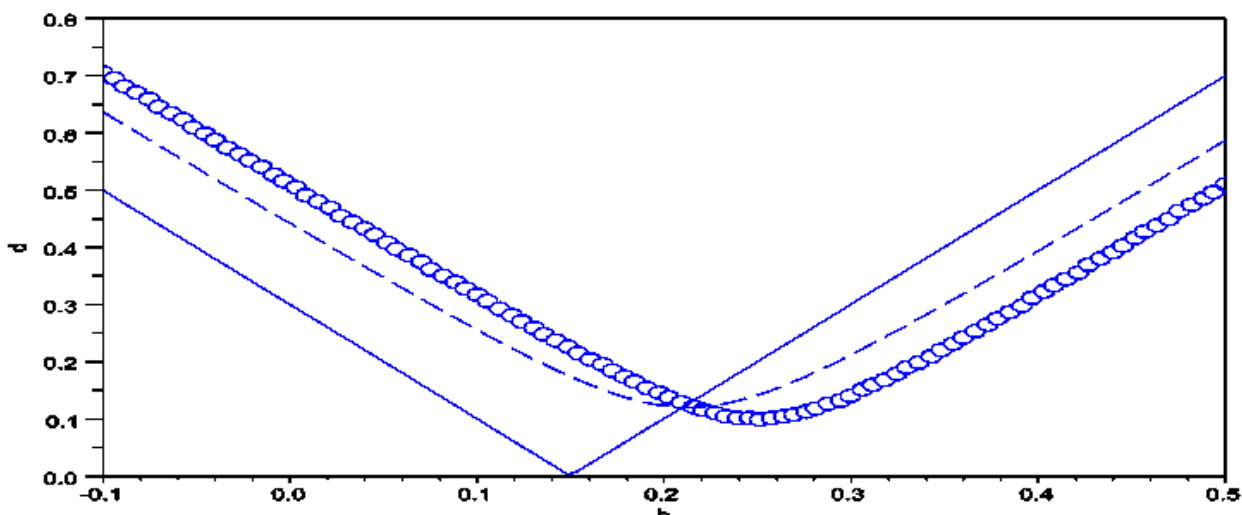


Fig-1. $n=1$ transition curve, Eq. (19) for $f_1 = f_0 = 0$, where the thick line represents $\alpha = 0$, dashed line is for $\alpha = 0.5$ and the circle line represents $\alpha = 1$. The figure is obtained using scilab software.

Similarly we may obtain approximations for other transition curves. For example, after [5] we may obtain an expression for the $n=0$ transition curve by starting with the ansatz

$$x = \beta \cos t + \lambda \sin t + \eta + \dots \tag{20}$$

Just as we did before, the $n=0$ transition curve is expressed as

$$b^3 + [2\xi c - 2\zeta - (f_1 + f_0)]b^2 + \left[\left(\sqrt{1-\zeta^2} - c\sqrt{1-\xi^2} \right)^2 + f_1(\zeta - \xi c) + f_0(\zeta - \xi c) + \zeta^2 + (\xi c)^2 + f_1 f_0 - 2\zeta \xi c - \frac{d^2}{2} \right] b + [f_1 + \zeta - \xi c] \frac{d^2}{2} = 0 \tag{21}$$

Setting $k = 2$, we obtain the $n=0$ transition curve for Eq. (10) as

$$2b^3 + (4(\xi c - 1) - 2(f_1 + f_0))b^2 + 2(c^2 - \xi c(f_1 + f_0) + (f_1 + f_0) + f_1 f_0 - 2\zeta c + 1 - d^2)b + (f_1 - \xi c + 1)d^2 = 0 \tag{22}$$

where $\xi = \cos \frac{\alpha\pi}{2}$ and $\zeta = \cos \frac{(k-2)\pi}{2}$. See Figure 4 where Eq. (22) is displayed for various values of

α, f_1 and f_0 . As was noted in Rand, et al. [5] the transition curve does not change much for $\alpha \in [0, 1]$, but as f_1, f_0 increases from zero we observe an increase in the value of the parametric forcing amplitude d for $\alpha \in [0, 1]$.

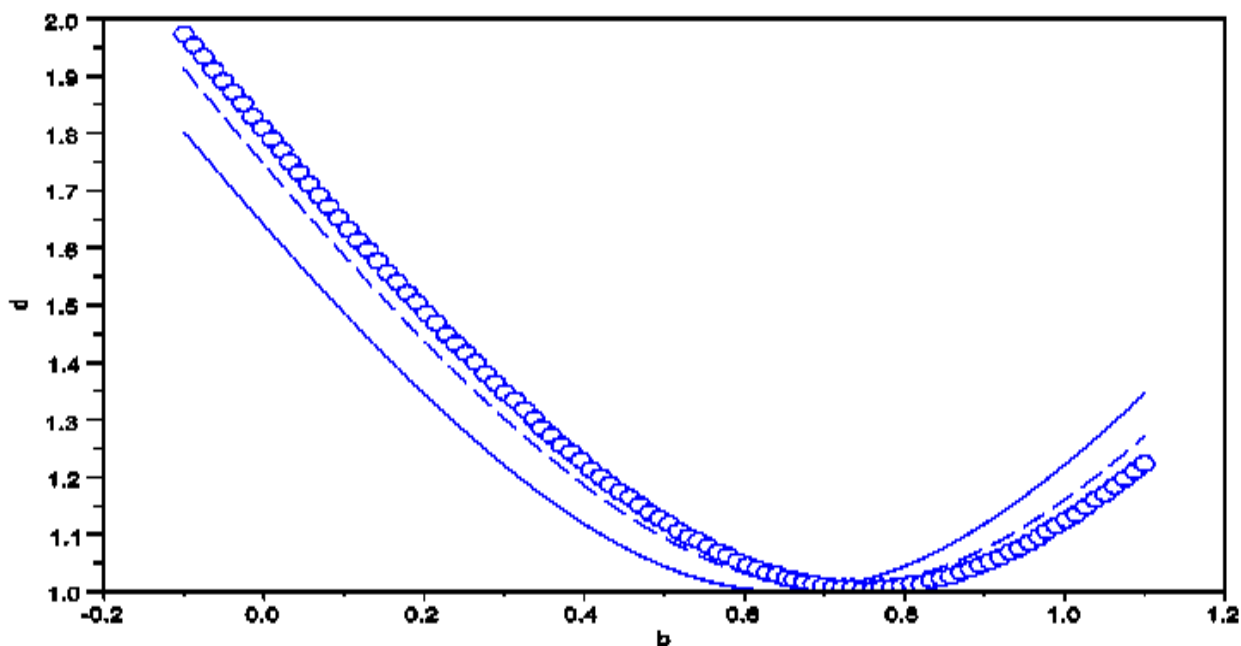


Fig-2. $n=1$ transition curve, Eq. (19) for $f_1 = f_0 = 0.5$, where the thick line represents $\alpha = 0$, dashed line is for $\alpha = 0.5$ and the circle line represents $\alpha = 1$. The figure is obtained using scilab software.

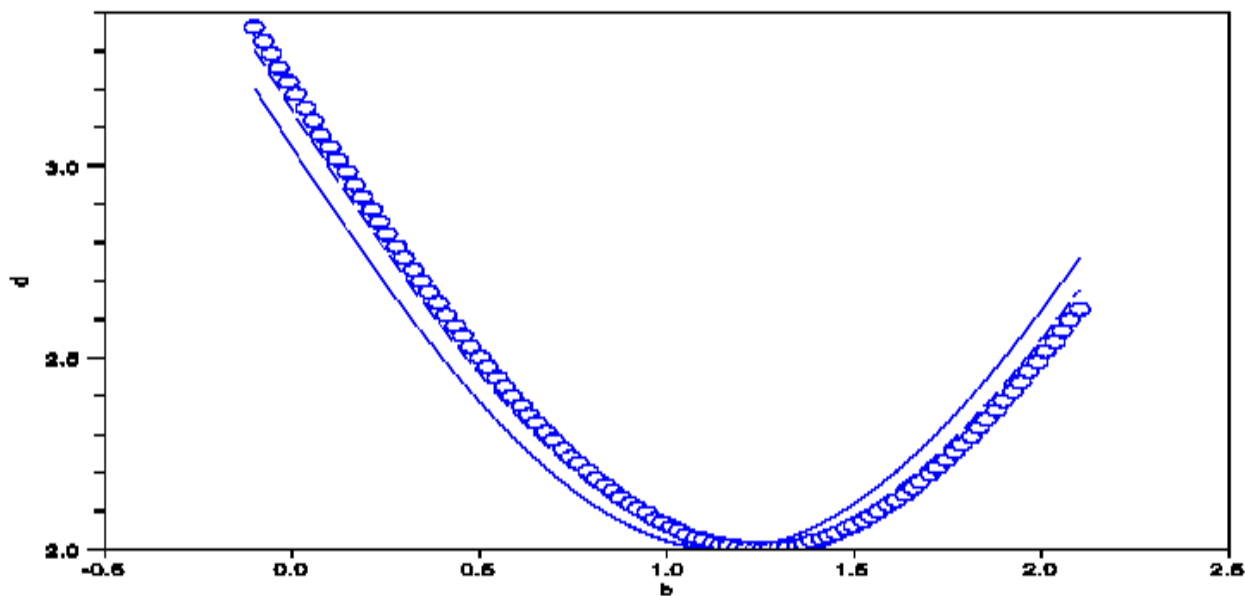


Fig-3. $n=1$ transition curve, Eq. (19) for $f_1 = f_0 = 1$, where the thick line represents $\alpha = 0$, dashed line is for $\alpha = 0.5$ and the circle line represents $\alpha = 1$. The figure is obtained using scilab software.

4. APPLICATION OF HPM

The basics of the HPM can be found in [14-21].

Consider the multi-order fractionally damped and forced Duffing-Mathieu equation given by

$$D_t^{2\alpha} x(t) + cD_t^\alpha x(t) + (b + d \cos vt)x(t) + \phi x(t)^3 = F_0 \cos jt + F_1 \sin jt$$

$$x(0) = p, x^\alpha(0) = q \tag{23}$$

According to the HPM, we construct a homotopy of the form,

$$H(X, p) = L(X) - L(X_0) + pL(X_0) + p[N(X) - f(r)] = 0 \tag{24}$$

where the given fractional DE above has the general form,

$$L(X) + N(X) - f(r) = 0 \tag{25}$$

In view of the HPM, we can write the solution of (25) as a power series of the form,

$$X = X_0 + pX_1 + \dots \tag{26}$$

Then letting $p = 1$, we obtain the solution to (25) as

$$x(t) = \lim_{p \rightarrow 1} X = X_0 + X_1 + \dots \tag{27}$$

Now from (23), we can take,

$$\begin{aligned} L(X) &= D^{2\alpha} x(t) + cD^\alpha x(t) + bx(t), N(X) = \phi x(t)^3 \\ f(r) &= F_0 \cos jt + F_1 \sin jt - dx(t) \cos vt \end{aligned} \tag{28}$$

From (26) and (24), we obtain,

$$\begin{aligned} D^{2\alpha} X + cD^\alpha X + bX - D^{2\alpha} X_0 - cD^\alpha X_0 - bX_0 + p[D^{2\alpha} X_0 + cD^\alpha X_0 + \delta X_0] \\ + p[\phi X^3 - F_0 \cos jt - F_1 \sin jt + dx(t) \cos vt] = 0 \end{aligned} \tag{29}$$

Substituting (26) into (29) yields

$$\begin{aligned} D^{2\alpha} (X_0 + pX_1 + \dots) + cD^\alpha (X_0 + pX_1 + \dots) + b(X_0 + pX_1 + \dots) \\ - D^{2\alpha} X_0 - cD^\alpha X_0 - bX_0 + p[D^{2\alpha} X_0 + cD^\alpha X_0 + bX_0] \\ + p[\phi(X_0^3 + 3pX_0^2 X_1 + \dots) - F_0 \cos jt - F_1 \sin jt + dx(t) \cos vt] = 0 \end{aligned} \tag{30}$$

Equating the powers of p to zero in (30) we have,

$$p^0 : D^{2\alpha} X_0 + cD^\alpha X_0 + bX_0 = 0 \tag{31a}$$

$$p^1 : D^{2\alpha} X_1 + cD^\alpha X_1 + bX_1 = -\phi X_0^3 - D^{2\alpha} X_0 - cD^\alpha X_0 - bX_0 + F_0 \cos jt + F_1 \sin jt - dX_0 \cos vt \tag{31b}$$

One may obtain other higher order terms if there is need for that, for this work we have no need for that.

The general solution to (31a) is given as,

$$X_0 = A_0 \exp(m_1 t) + B_0 \exp(m_2 t) \tag{32}$$

where,

$$m_1 = \left[\frac{1}{2} (\sqrt{c^2 - 4b} - c) \right]^{\frac{1}{\alpha}}, m_2 = \left[-\frac{1}{2} (\sqrt{c^2 - 4b} + c) \right]^{\frac{1}{\alpha}} \tag{33}$$

$$A_0 = \frac{pm_2^\alpha - q}{m_2^\alpha - m_1^\alpha}, B_0 = \frac{q - pm_1^\alpha}{m_2^\alpha - m_1^\alpha}$$

From (31b) and (32), we obtain,

$$X_1 = A_1 \exp(m_1 t) + B_1 \exp(m_2 t) + X_{1P} \tag{34}$$

where,

$$A_1 = \frac{(3m_1)^\alpha G_1 + \dots + (m_2 - ij)^\alpha G_8 + j^\alpha \left[G_9 \cos\left(jt + \frac{\alpha\pi}{2}\right) + G_{10} \sin\left(jt + \frac{\alpha\pi}{2}\right) \right] - m_2^\alpha [G_1 + \dots + G_9]}{m_2^\alpha - m_1^\alpha}$$

$$B_1 = \frac{m_1^\alpha [G_1 + \dots + G_9] - \left[(3m_1)^\alpha G_1 + \dots + (m_2 - ij)^\alpha G_8 + j^\alpha \left[G_9 \cos\left(jt + \frac{\alpha\pi}{2}\right) + G_{10} \sin\left(jt + \frac{\alpha\pi}{2}\right) \right] \right]}{m_2^\alpha - m_1^\alpha}$$

$$X_{1P} = G_1 \exp(3m_1 t) + G_2 \exp(2m_1 + m_2) t + G_3 \exp(m_1 + 2m_2) t + G_4 \exp(3m_2) t + G_5 \exp(m_1 + iv) t$$

$$G_6 \exp(m_1 - iv) t + G_7 \exp(m_2 + iv) t + G_8 \exp(m_2 - iv) t + G_9 \cos jt + G_{10} \sin jt \tag{35}$$

and,

$$G_1 = \frac{-\beta A_0^3}{(3m_1)^{2\alpha} + c(3m_1)^\alpha + b}, G_2 = \frac{-3\beta A_0^2 B_0}{(2m_1 + m_2)^{2\alpha} + c(2m_1 + m_2)^\alpha + b}, G_3 = \frac{-3\beta B_0^2 A_0}{(m_1 + 2m_2)^{2\alpha} + c(m_1 + 2m_2)^\alpha + b},$$

$$G_4 = \frac{-\beta B_0^3}{(3m_2)^{2\alpha} + c(3m_2)^\alpha + b}, G_5 = \frac{-dA_0}{2[(m_1 + iv)^{2\alpha} + c(m_1 + iv)^\alpha + b]}, G_6 = \frac{-dA_0}{2[(m_1 - iv)^{2\alpha} + c(m_1 - iv)^\alpha + b]},$$

$$G_7 = \frac{-dB_0}{2[(m_2 + iv)^{2\alpha} + c(m_2 + iv)^\alpha + b]}, G_9 = \frac{F_0 \left(j^{2\alpha} \cos \alpha\pi + cj^\alpha \cos \frac{\alpha\pi}{2} + b \right) - F_1 \left(j^{2\alpha} \sin \alpha\pi + cj^\alpha \sin \frac{\alpha\pi}{2} \right)}{\left(j^{2\alpha} \cos \alpha\pi + cj^\alpha \cos \frac{\alpha\pi}{2} + b \right)^2 + \left(j^{2\alpha} \sin \alpha\pi + cj^\alpha \sin \frac{\alpha\pi}{2} \right)^2}$$

$$G_{10} = \frac{F_1 \left(j^{2\alpha} \cos \alpha\pi + cj^\alpha \cos \frac{\alpha\pi}{2} + b \right) + F_0 \left(j^{2\alpha} \sin \alpha\pi + cj^\alpha \sin \frac{\alpha\pi}{2} \right)}{\left(j^{2\alpha} \cos \alpha\pi + cj^\alpha \cos \frac{\alpha\pi}{2} + b \right)^2 + \left(j^{2\alpha} \sin \alpha\pi + cj^\alpha \sin \frac{\alpha\pi}{2} \right)^2}, G_8 = \frac{-dB_0}{2[(m_2 - iv)^{2\alpha} + c(m_2 - iv)^\alpha + b]} \tag{36}$$

If two terms are sufficient enough, we can write the solution to (24) using (27) and (32)-(36).

If not we can obtain higher order approximations via (31).

5. DISCUSSION

In the case of the $n=1$ transition curves (see Eq. (19) and Figs. 1,2, and 3), we observed that in as much as a change in the order α of the fractional derivative affects the shape and location of the transition curves [5] the introduction of external forcing enhances these effects and the rate at which they occur. We note that as the external forcing is increased, the transition curves become more parabolic in shape. After [5] we can characterize these effects through the location of the lowest point on the transition curves, representing the minimum quantity of parametric forcing amplitude needed to produce instability. We denote this minimum value of d , for a given α as d_{\min} .

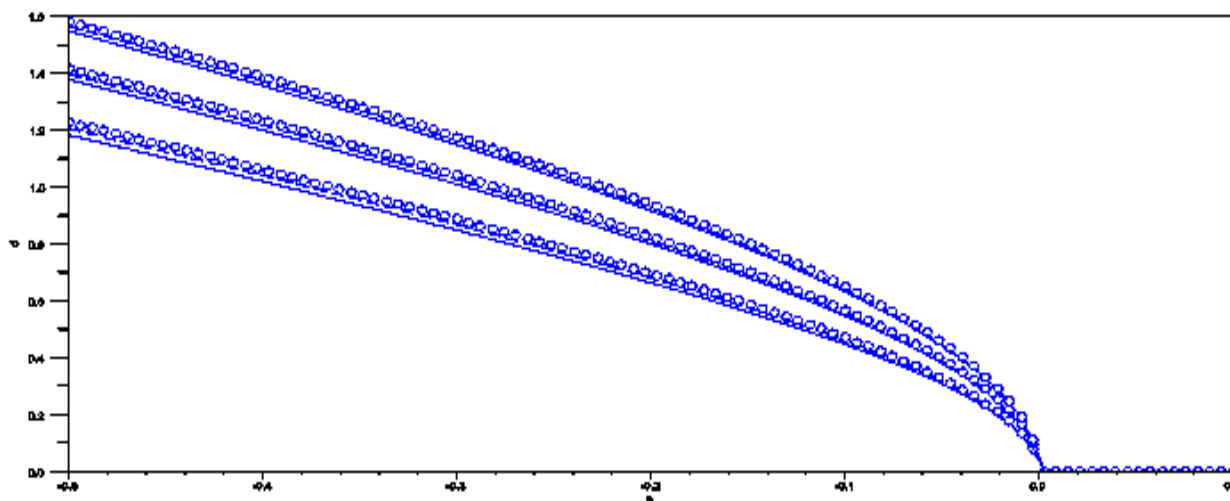


Fig-4. $n=0$ transition curve, Eq. (22) for $c = 0.1$. The three leftmost curves corresponds to $f_1 = f_0 = 0$. The middle curves corresponds to $f_1 = f_0 = 0.5$. The rightmost curves corresponds to $f_1 = f_0 = 1$. Where the thick lines represents $\alpha = 0$, dashed lines is for $\alpha = 0.5$ and the circle lines represents $\alpha = 1$. The figure is obtained using scilab software.

To obtain an expression for d_{\min} in the presence of external forces, we may obtain the slope of the transition curve by differentiating Eq. (19) with respect to d , requiring this slope to be infinite after [5] we obtain

$$d_{\min} = (f_0 - f_1) \pm \sqrt{\frac{c^2}{2^{2\alpha-2}} \sin^2 \frac{\alpha\pi}{2}} \tag{37}$$

Similarly we may obtain expressions for $f_{1\min}$ and $f_{0\min}$ by differentiating Eq. (19) with respect to f_1 and f_0 respectively. We find

$$f_{1\min} = (f_0 - d) \pm \sqrt{(f_0 - d)^2 - f_0(f_0 - 2d) - d^2 + \frac{c^2}{2^{2\alpha-2}} \sin^2 \frac{\alpha\pi}{2}} \tag{38}$$

$$f_{0\min} = (f_1 + d) \pm \sqrt{(f_1 + d)^2 - f_1(f_1 + 2d) - d^2 + \frac{c^2}{2^{2\alpha-2}} \sin^2 \frac{\alpha\pi}{2}} \tag{39}$$

See Fig. 5 where d_{\min} is plotted as a function of α for no or equal external forcing amplitude. The greatest effect is observed where this curve achieves its maximum [5] shown by a toggle in Fig. 5. Following Rand, et al. [5] we denote the corresponding value of α as α_* . Differentiating Eq. (37) with respect to α and setting

$dd_{\min}/d\alpha$ equal to zero, we may obtain an expression for α_* as

$$\alpha_* = \frac{2}{\pi} \arctan \frac{\pi}{2 \ln 2} \approx 0.74 \tag{40}$$

The same result (40) is also obtained for (38) and (39) following the same procedure. We note here that the value

α_* remains unchanged for all $f_1 f_0$. Referring to the corresponding value of d_{\min} as d_{\min}^* , we obtain

$$d_{\min}^* \approx (f_0 - f_1) \pm \sqrt{1.2078c^2} \tag{41}$$

Similarly

$$f_{1_{\min}}^* \approx (f_0 - d) \pm \sqrt{(f_0 - d)^2 - f_0(f_0 - 2d) - d^2 + 1.2078c^2} \tag{42}$$

$$f_{0_{\min}}^* \approx (f_1 + d) \pm \sqrt{(f_1 + d)^2 - f_1(f_1 + 2d) - d^2 + 1.2078c^2} \tag{43}$$

We can deduce from (41) that d_{\min}^* varies directly to c as long as $f_1 = f_0$ or $f_1 = f_0 = 0$. For constant c ,

$d_{\min}^* > 0$, if $f_1 < f_0$ and $d_{\min}^* < 0$, if $f_1 > f_0$, as displayed in Fig. 6. From (42), we observe that as d increases,

$f_{1_{\min}}^*$ decreases. From (43), we observe also that as d increases, $f_{0_{\min}}^*$ increases.

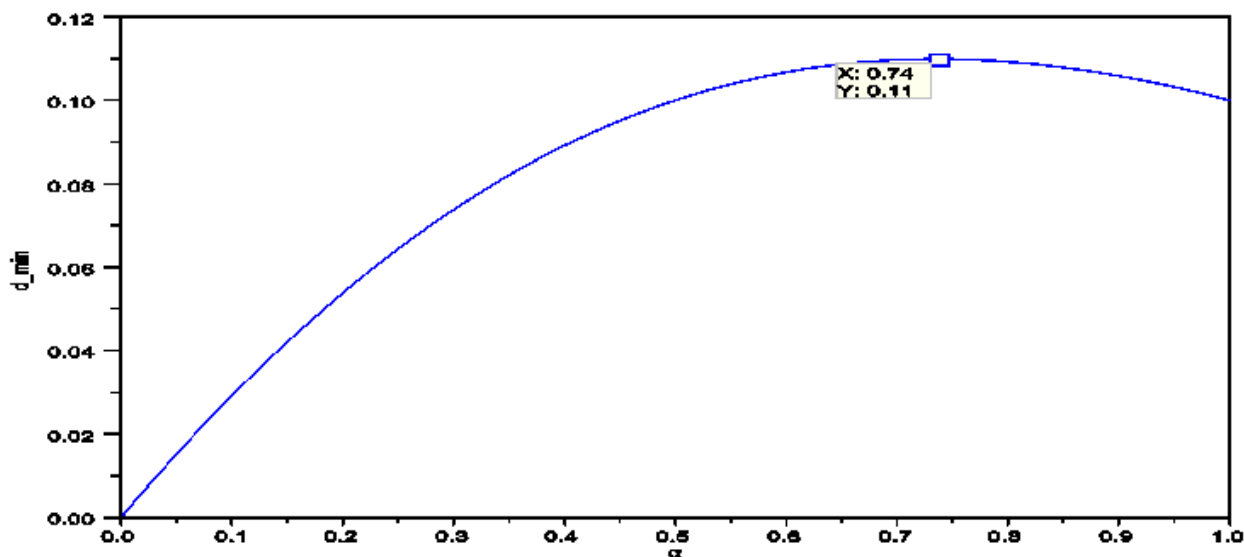


Fig-5. Plot of d_{\min} , the minimum quantity of parametric forcing amplitude required to produce instability, as a function of fractional derivative order α , Eq. (37). The figure is obtained using scilab software.

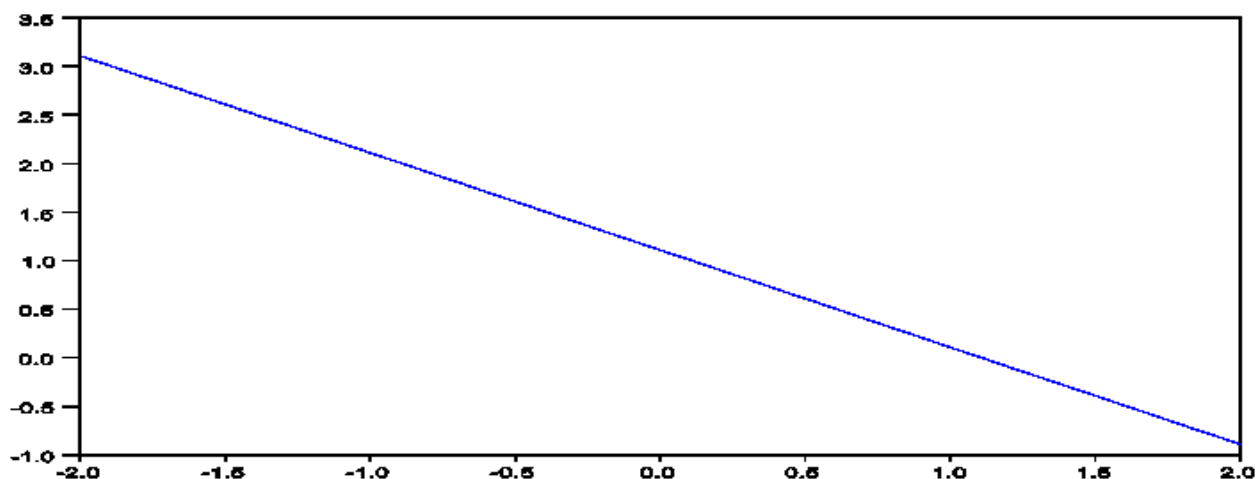


Fig-6. Plot of d_{\min}^* , the corresponding value of d_{\min} at α_* as a function of the external forcing amplitude f_1 , Eq. (41) for $f_0=1$. The figure is obtained using scilab software.

As was observed in Rand, et al. [5] the damping effect of the fractional derivative term in Eq. (11), for $0.5 < \alpha < 1$, is greater than that of the non-fractional damped Mathieu equation which corresponds to setting $\alpha = 1$ in Eq. (11), this remains true even in the presence of external forces.

In contrast to non-fractional damping, fractional damping also moves the lowest point on the transition curve in a horizontal direction, see Fig. 1, thereby effectively changing the resonant value of b Rand, et al. [5]. In the presence of external forcing, the movement of this lowest point becomes faster and the detachment of resonant tongues from the horizontal line becomes faster too.

However, the values of the parametric forcing amplitude d increases noticeably with the introduction of increasing external forcing in the case of $n=0$ transition curves (see Eq. (22) and Fig. 4).

6. CONCLUSION

In this paper we have investigated the externally excited fractional Mathieu equation (10) using the harmonic balance method after [5]. We obtained explicit approximate expressions for the $n=1$ and $n=0$ transition curves separating regions of stability from regions of instability in Eq. (10). We showed that by adding external forcing to Eq. (11) and changing the value of the order of the fractional derivative, α , the shape and location of the $n=1$ transition curve changes rapidly compared to when there is no external forcing. We also showed that the greatest value α_* of the order of the fractional derivative α for which the minimum quantity of parametric forcing d necessary to produce instability is given, remains unchanged even in the presence of external excitation. We obtained an approximate analytical solution to the multi-order fractional Mathieu equation introduced and some special cases of the considered equation. Future works may investigate the effect of delay and nonlinearity on the multi-order fractional Mathieu equation.

Funding: This study received no specific financial support.

Competing Interests: The author declares that there are no conflicts of interests regarding the publication of this paper.

REFERENCES

- [1] J. I. Nwamba, "Delayed Mathieu equation with fractional order damping: An approximate analytical solution," *International Journal of Mechanics and Applications* vol. 3, pp. 70-75, 2013.
- [2] E. Mathieu, "Memoire sure le mouvement vibratoire d'une membrane de forme Elliptique," *Journal de Mathématiques Pures et Appliquées*, vol. 13, pp. 137-203, 1868.
- [3] A. Nayfeh and D. T. Mook, *Nonlinear oscillations*. New York: Wiley, 1979.
- [4] R. H. Rand, "Lecture notes on nonlinear vibrations (version 53). Retrieved from <http://audiophile.tam.cornell>," 2012.
- [5] R. H. Rand, S. M. Sah, and M. K. Suchorsky, "Fractional mathieu equation," *Communications in Nonlinear Science and Numerical Simulation*, vol. 15, pp. 3254-3262, 2010.
- [6] A. Ebaid, D. M. M. Elsayeed, and M. D. Aljoufi, "Fractional calculus model for damped Mathieu equation: Approximate analytical solution," *Applied Mathematical Sciences*, vol. 6, pp. 4075-4080, 2012.
- [7] O. A. Taiwo and O. S. Adetunde, "Approximation of multi-order fractional differential equations by an iterative decomposition method," *American Journal of Engineering Science and Technology Research*, vol. 1, pp. 10-18, 2013.
- [8] I. K. Hanan, "The homotopy analysis method for solving multi-fractional order integro-differential equations," *J. Al-Nahrain Univ.*, vol. 14, pp. 139-143, 2011.
- [9] R. L. Bagley and P. J. Torvik, "A theoretical basis for the application of fractional calculus to viscoelasticity," *Journal of Rheology*, vol. 27, pp. 201-210, 1983.
- [10] I. N. Joshua, "Joshua Ikechukwu Nwamba: Exact and explicit approximate solutions to the multi-order fractional burgers-poisson and fractional burgers-poisson equations," *Applied and Computational Mathematics*, vol. 2, pp. 78-85, 2013.
- [11] H. M. Srivasta and R. K. Saxena, "Operators of fractional integration and their applications," *Applied Mathematics and Computation*, vol. 118, pp. 1-52, 2001.
- [12] R. Hilfer, "Applications of fractional calculus in physics." Retrieved from <http://cict.umcc.cu/repositorioinstitucional/Matem%C3%A1tica/16-Medida%20e%20Integraci%C3%B3n/Fractional%20Calculus/Applications%20of%20Fractional%20Calculus%20in%20Physics.pdf>, 2000.
- [13] I. Podlubny, *Fractional differential equations*. San Diego, California: Academic Press, 1999.
- [14] J. H. He, "Homotopy perturbation technique," *Computer Methods in Applied Mechanics and Engineering*, vol. 178, pp. 257-262, 1999.
- [15] J. H. He, "An elementary introduction to the homotopy perturbation method," *Computers and Mathematics with Applications*, vol. 57, pp. 410-412, 2009.
- [16] J. H. He, "The homotopy perturbation method for nonlinear oscillators with discontinuities," *Applied Mathematics and Computation*, vol. 151, pp. 287-292, 2004.
- [17] J. H. He, "Homotopy perturbation method: A new nonlinear analytical technique," *Applied Mathematics and Computation*, vol. 137, pp. 73-79, 2003.
- [18] J. H. He, "Recent development of the homotopy perturbation method," *Topological Methods in Nonlinear Analysis*, vol. 31, pp. 205-209, 2008.
- [19] B. Raftari, "Application of he's homotopy perturbation method and variational iteration method for nonlinear partial integro-differential equations," *World Applied Sciences Journal*, vol. 7, pp. 399-404, 2009.

- [20] C. Chum and R. Sakthivel, "Homotopy perturbation technique for solving two-point boundary value problems-comparison with other methods," *Computer Physics Communications*, vol. 181, pp. 1021-1024, 2010.
- [21] M. M. Ghasemi, "Numerical solution of the nonlinear integro-differential equations: Wavelet-Galerkin method and homotopy perturbation method," *Applied Mathematics and Computation*, vol. 188, pp. 450-455, 2007.

Views and opinions expressed in this article are the views and opinions of the author(s), International Journal of Mathematical Research shall not be responsible or answerable for any loss, damage or liability etc. caused in relation to/arising out of the use of the content.